Composites Science and Technology 110 (2015) 217–223

Contents lists available at ScienceDirect

Composites Science and Technology

journal homepage: www.elsevier.com/locate/compscitech

Preparation and interaction study between fullerene and graphene in a polymeric matrix

Valeria Alzari [a], Gerardo Zaragoza-Galán [b,c], Daniele Nuvoli [a], Javier Illescas [a], Ernesto Rivera [b,*], Vanna Sanna [a], Erika Conca [d], Alberto Mariani [a,*]

[a] Dipartimento di Chimica e Farmacia, Università degli Studi di Sassari, e unità locale INSTM, via Vienna 2, 07100 Sassari, Italy
[b] Instituto de Investigaciones en Materiales, Universidad Nacional Autónoma de México, Ciudad Universitaria, C.P. 04510 D.F. México, Mexico
[c] Facultad de Ciencias Químicas, Universidad Autónoma de Chihuahua, Campus Universitario 2, Apartado Postal 669, Chihuahua 31125, Mexico
[d] Dipartimento di Scienze Chimiche e Geologiche ed INSTM, Università di Cagliari, 09042 Monserrato (Ca), Italy

ARTICLE INFO

Article history:
Received 17 September 2014
Received in revised form 13 January 2015
Accepted 13 February 2015
Available online 25 February 2015

Keywords:
Nanocomposites
A. Nano particles
A. Polymer-matrix composites (PMCs)
A. Polymers
A. Frontal polymerization

ABSTRACT

Defect-free graphene is easily obtained by the liquid dispersion method, without any chemical manipulation. Tetraethylene glycol diacrylate (TEGDA) is used as liquid medium in which the above nanofiller is dispersed alone or together with fullerene C60. TEGDA is used because of its good dispersion properties and as a monomer to be eventually polymerized, thus directly obtaining the corresponding polymer nanocomposites. Polymerization is performed by using both the classical or the frontal polymerization, Moreover, polymeric films were also prepared. The interaction between the two fillers and the influence of the synthetic techniques on material properties are deeply studied. The optical properties of the obtained nanocomposites are analyzed by absorption and fluorescence spectroscopy. Graphene containing materials show absorption at ca. 280 nm and exhibited significant emission in the range between 600 and 800 nm. In contrast, fullerene containing materials do not show any fluorescence, which can be attributed to a charge transfer phenomenon from graphene to fullerene C60.

1. Introduction

Graphene-based materials, including zero-dimensional (0D) fullerenes, one-dimensional (1D) carbon nanotubes (CNTs), two-dimensional (2D) graphene, and three-dimensional (3D) graphite, are of particular interest because of their exceptional electrical and mechanical properties [1,2]. Graphene, a monolayer of sp^2 hybridized carbon atoms bonded in a hexagonal lattice, is formally the parent of all the graphitic carbon forms [1,3–5]. Our research group improved a method to obtain graphene initially proposed by Hernandez et al. [6] that involves the use of ultrasounds in order to exfoliate graphite, without any chemical manipulation and without using graphite oxide [7–12], which generally results in considerable damaging of the graphene electronic structure [13]. In addition, in order to synthesize polymeric nanocomposites containing graphene, our research group obtained graphene directly in the monomer [12–14] thus allowing for the direct, in situ polymerization of the graphene/monomer dispersion. On this respect, graphene-based polymer composites are very attractive materials that can be used for packaging for food, medicine, electronics [15], energy storage [16], electrically conductive polymers [17], making transparent conductive electrode for solar cells [18], and electrochromic devices [19]. Also photovoltaics based on fullerene C60 derivatives is one of the most attractive research areas in polymer science due to the advantages offered by these molecules for solar energy conversion [20–25]. However, fullerene C60 has some drawbacks because of its poor solubility in organic solvents [26] and its main absorption in the UV region. It is well known that a wide (UV and visible) absorption range is desirable for organic photovoltaics [20,27–33]. Frontal Polymerization (FP) is a polymerization technique that allows the conversion of a monomer into a polymer by formation and consequent propagation of a localized reaction zone [7,8,11,34–52]. The resulting polymerization front is able to self-sustain and propagate along the whole reactor. If compared with the classical polymerization (CP), FP has many advantages: shorter reaction time, low-energy consumption, easy and simple protocols, and affords obtaining materials that often have better properties than those obtained by CP. Recently, poly (tetraethylene glycol diacrylate) (PTEGDA) has shown to be an interesting candidate to obtain few-layer graphene in a reactive medium [12,14]. In this work, new polymeric nanocomposite

* Corresponding authors.
E-mail addresses: riverage@unam.mx (E. Rivera), mariani@uniss.it (A. Mariani).

http://dx.doi.org/10.1016/j.compscitech.2015.02.011
0266-3538/

materials based on PTEGDA matrix containing graphene and fullerene were synthesized. In particular, the nanocomposite materials were obtained in three different ways: by FP, by CP and by film casting. In addition, the interaction between graphene and fullerene on polymeric nanocomposite properties was deeply studied, by analyzing the thermal, morphological and optical properties [53–55] of the obtained materials.

2. Experimental

2.1. Materials and methods

Tetraethylene glycol diacrylate (TEGDA, M_W = 302.32, d = 1.11 g/mL) and graphite powder were purchased from Sigma–Aldrich and used as received. Trihexyltetradecyl phosphonium persulfate (TETDPPS) was used as the radical initiator and was synthesized according to the method described in the literature [56]. Fullerene C60 was purchased from Buchi company and used as received.

2.2. Preparation and characterization of graphene and graphene/fullerene dispersions in TEGDA

To prepare a graphene dispersion, 5 wt.% of graphite powder was added to TEGDA, placed into a tubular plastic reactor (i.d. 15 mm) and ultrasonicated (Ultrasound bath EMMEGI, 0.55 kW, water temperature ≈40 °C) for 24 h. Then, the dispersion was centrifuged for 30 min at 4000 rpm; finally, the gray-to-black liquid phase containing graphene was recovered. The concentration of the dispersion, determined by gravimetry after filtration through polyvinylidene fluoride filters (pore size 0.22 μm), was found to be 5.8 mg/mL; the absorption coefficient, obtained by UV–vis analysis, was 50 mL/mg^{-1} m^{-1}. Suitable amounts of fullerene C60 were homogeneously dispersed in the above TEGDA/graphene dispersion in order to obtain various graphene/fullerene ratios (Table 1). Each dispersion was divided into three parts, one used to synthesize the corresponding nanocomposite material as film, and the other two to synthesize the bulk materials through FP and CP. In each dispersion, TETDPPS initiator was added (1 wt.% respect to the monomer). The graphene dispersion was analyzed by UV–VIS spectroscopy, using a Hitachi U-2010 spectrometer (1 mm cuvette) to determine the concentrations of the diluted dispersions. Transmission electron microscopy (TEM) images were recorded on a Hitachi H-7000 instrument running with a thermoionic W gun at 125 KV, and equipped with a AMT DVC (2048 × 2048 pixel) CCD Camera. Prior to observation, a drop of the TEGDA-based suspension was sonicated, deposited on a copper grid and dried at room temperature.

2.3. Synthesis of polymeric nanocomposite materials

2.3.1. Classical polymerization

A common glass test tube (inner diameter = 1.5 cm, length = 16 cm) was filled with the reacting mixture (Table 1). The classical polymerization was performed by keeping the tube immersed in an oil bath at 80 °C for 2 h.

2.3.2. Frontal polymerization

A common test tube (inner diameter = 1.5 cm, length = 16 cm) was filled with the same reacting mixtures as above (Table 1). A K-type thermocouple was located at about 1 cm from the bottom of the tube and connected to a digital temperature recorder (Delta Ohm 9416, ±1.0 °C), to record the front temperature, T_{max}. FP started by heating the external wall of the tube in correspondence of the upper surface of the monomeric mixture. The position of the front (easily visible through the glass wall of test tubes) against time was also monitored in order to determine the front velocity, V_f. T_{max} and V_f reproducibility was always within ±10 °C and ±0.5 mm, respectively.

2.3.3. Films

The polymerization of a few drops of mixture was performed on silicon wafers (3 cm × 3 cm) located on a heating plate at ca. 100 °C for some minutes (Table 1).

2.4. Characterization of polymeric nanocomposites

The polymeric nanocomposite films were characterized by thermogravimetric analysis (TGA) and differential scanning calorimetry (DSC) under inert atmosphere. TGA was carried out in a Hi-Res TGA 2950 Instrument, from 0 to 700 °C under nitrogen atmosphere. Differential scanning calorimetry (DSC) measurements were conducted in a DSC 2910 TA Instrument. For each sample, two consecutive scans were carried out from −85 to 250 °C with a heating rate of 10 °C min, under nitrogen atmosphere. The morphological characterization was investigated by using a Zeiss

Table 1
Composition and synthetic technique used for nanocomposite materials; T_{max} and V_f values for FP samples; T_g and T_{on} values for FP and CP samples.

Sample code	Polymerization method	Graphene:fullerene	T_{max} (°C)	V_f (cm/min)	T_g (°C)	T_{on} (°C)
FP(0/0)	FP	0:0	224	2.4	30	396
CP(0/0)	CP				28	393
FILM(0/0)	Film					
FP(0/1)	FP	0:1	217	1.6	31	379
CP(0/1)	CP				30	382
FILM(0/1)	Film					
FP(1/0)	FP	1:0	171	0.8	30	420
CP(1/0)	CP				29	417
FILM(1/0)	Film					
FP(1/1)	FP	1:1	204	1.2	30	417
CP(1/1)	CP				29	419
FILM(1/1)	Film					
FP(1/2.5)	FP	1:2.5	222	2.0	30	413
CP(1/2.5)	CP				29	386
FILM(1/2.5)	Film					
FP(2.5/1)	FP	2.5:1	205	1.2	30	381
CP(2.5/1)	CP				29	418
FILM(2.5/1)	Film					

EVO LS 10 ESEM, in high vacuum modality with secondary electron detector. Before the examination, the samples were mounted on a carbon stubs, coated with a carbon film using an auto-carbon coater evaporator (Agar Instruments) and observed with back scattered electron detector in high vacuum modality. The microanalysis was carried out using a Zeiss EVO LS 10 ESEM with an energy dispersive system (EDS), Inca X-Act (Oxford Instruments). FTIR spectrum of the obtained nanocomposite materials was carried out on a Spectrum 100 (Perkin Elmer) spectrometer in solid state. The absorption spectra of the modified fullerene in solid state or thin film were recorded on a Varian Cary 1 Bio UV/vis spectrophotometer. Fluorescence spectra corrected for the emission detection were recorded on a Photon Technology International LS-100 steady-state fluorimeter having a continuous Ushio UXL-75Xe Xenon arc lamp and a PTI 814 photomultiplier detection system. Each film sample was excited at 280 nm using a front face configuration.

3. Results and discussion

The concentration of graphene, determined by gravimetry after filtration, was 5.8 mg/mL. The absorption coefficient found after UV–Vis analysis and construction of calibration curve, which shows a Lambert Beer behavior, was 50 mL mg^{-1} m^{-1}. This value was used in order to determine the actual concentration in the diluted dispersions. After fullerene addition (when needed), they were analyzed by TEM.

Fig. 1 shows three TEM micrographs related to the dispersion of graphene (A), fullerene (B) and graphene/fullerene (C). Fig. 1A was taken by analyzing the liquid dispersion containing graphene/TEGDA only. The image shows a large mono or few-layer graphene sheet. Its regular edges confirm that the ultrasonic process resulted in a good graphite exfoliation; more, it was not disruptive. On the other hand, Fig. 1B displays an image taken by TEM analysis of the dispersion constituted of fullerene only. The image confirms that also in this case a good dispersion of this material was achieved. Finally, in Fig. 1C the image of the mixture containing both graphene and fullerene is shown. This image confirms that both nanofillers are homogeneously dispersed in the monomer mixture.

T_{max} and V_f data of the FP samples are reported in Table 1. It is noteworthy that all samples containing graphene and/or fullerene are characterized by lower T_{max} and V_f as compared with the neat polymer. This is due to the dissipation of heat due to the presence of the inert filler. However, these parameters decrease as the content of graphene raises, while they increase with the amount of fullerene. The reasons for such a behavior, which is different from one nanofiller to the other, are not well understood and will be investigated in the future.

Morphological analysis was performed by SEM on both films and bulk polymers. The micrographs show a very homogeneous surface, which suggests that graphene and fullerene are well compatible with the polymeric matrix (Fig. 2).

Thermal analyses were carried out by using both DSC and TGA (Table 1). It was found that the presence of the nanofillers does not significantly influence the glass transition, with all T_g values being very close 29 °C. However, the data seem to indicate that FP samples are characterized by T_g's that are higher than those of the CP ones. However, even if this relation holds in all samples, the difference is too low to be really worth noting. In Fig. 3A the TGA curves of the FP samples are displayed. As it can be seen, all of them present a T_{on} above 380 °C. Again, the presence of graphene or fullerene does not influence this value. However, the effect of the nanofiller is clearly visible starting from ca. 420 °C (Fig. 3A, right image) thus suggesting that the interaction among graphene, fullerene and polymer matrix might influence the degradation of this latter in this temperature range. In particular, samples containing at least 0.035 wt.% graphene degradate faster than the others. These data are confirmed by the analyses performed on the CP samples (not shown).

Absorption and emission spectra of the nanocomposite films were performed in the solid state. In particular, absorption spectra of all samples show an intense absorption in the ultraviolet range, which is extended to the visible region, beyond 400 nm, especially in the samples containing fullerene C60 (Fig. 3B). This trend is more evident for FILM(0/1), which contains the highest fullerene C60 concentration. Sample FILM(1/0), which lacks of fullerene C60, does not show any remarkable absorption in the visible range of the spectrum. A well-defined shoulder at 280 nm was observed for samples containing different quantities of graphene. This shoulder is better structured in FILM(1/0), containing 0.07 wt.% of graphene, and its intensity decreases as the fullerene C60 content rises in the films. Fluorescence spectrum of sample containing 0.07 wt.% of graphene (FILM(1/0)) shows a well-structured band centered at 680 nm after excitation of the film at 280 nm (Fig. 3C). Emission of the sample is mainly due to graphene. Although graphene very often acts as acceptor and quencher [57] it shows a discrete fluorescence emission. We calculated the integration area of the emission in the range between 600 and 800 nm and assigned a value of 1 to the selected area. This value represents the maximum quantum yield of fluorescence of the samples. In this way, we were able to determine the relative fluorescence quantum yield of the other samples by comparison of the integrated area of

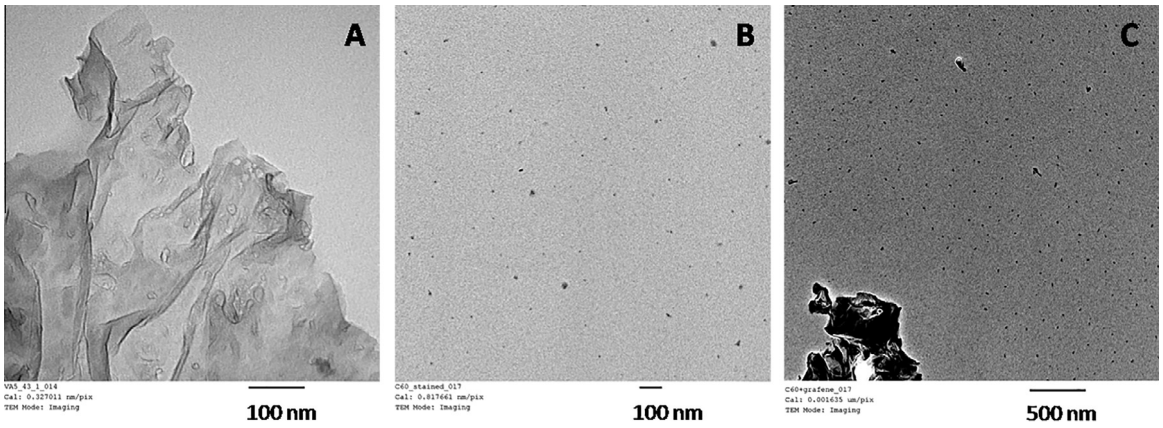

Fig. 1. TEM micrographs of: (A) graphene dispersion in TEGDA (0.033 wt.%); (B) fullerene dispersion in TEGDA (0.05 wt.%) and (C) graphene/fullerene dispersion in TEGDA (0.035/0.035 w/w; in order to distinguish both graphene and fullerene contrast has been increased).

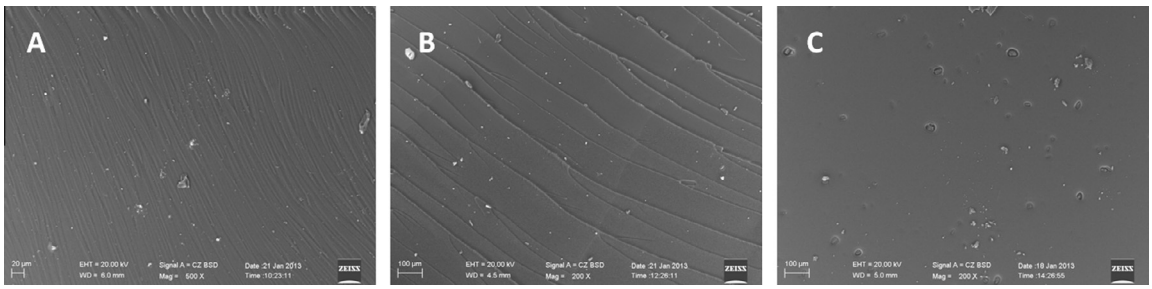

Fig. 2. SEM micrographs of some samples with the same composition (graphene/fullerene 1:2.5) synthesized by FP (A), CP (B) and as film (C).

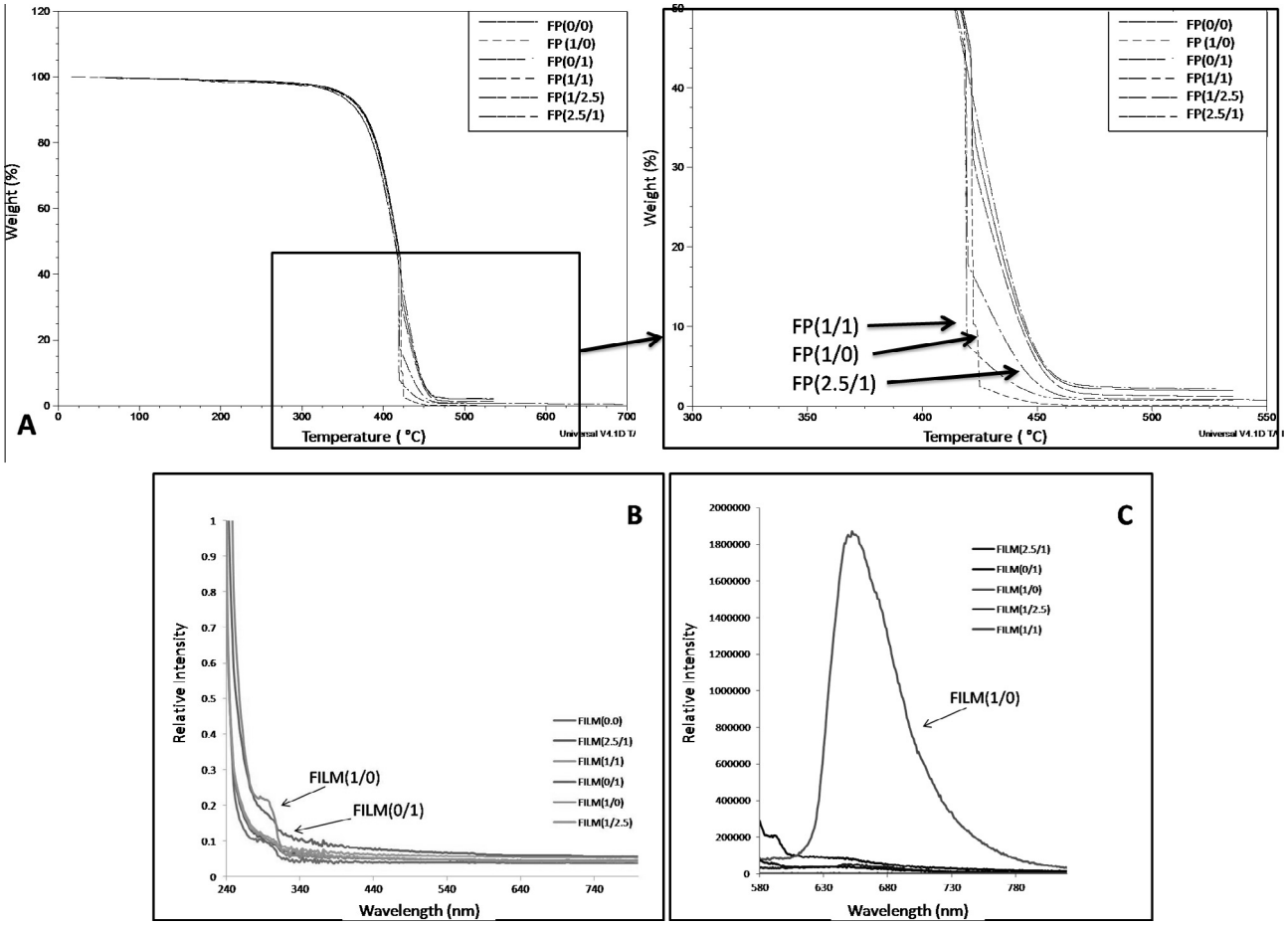

Fig. 3. (A) TGA curves of FP samples (on the right, a zoom of the thermographs shown on the left). (B) Absorption and (C) emission spectra of graphene/fullerene C60 polymer nanocomposite films.

Table 2
Relative quantum yield, relative fluorescence intensity and quenching degree of the samples (a.u.).

Simple code	Relative quantum yield[a]	Relative intensity[b]	Quenching (%)[b]
FILM(1/0)	1.0	100.0	0.0
FILM(2.5/1)	0.035	3.2	96.8
FILM(1/1)	0.0034	3.5	96.4
FILM(1/2.5)	0.032	0.3	99.6
FILM(0/1)	0.076	7.6	92.4

[a] In the emission range of 600–800 nm after excitation at 280 nm.
[b] Relative to FILM(1/0) fluorescence.

emission in this region for the corrected fluorescence spectra. The obtained results are shown in Table 2. It is important to notice that excitation of samples at other wavelengths does not result in any emission, which proves that fluorescence arises exclusively from graphene.

It is worth to point out that even samples containing small amounts of fullerene C60 exhibited very low fluorescence intensity. This is due to the quenching of graphene fluorescence by fullerene C60. To confirm these results we carried out some experiments starting at a very low fullerene C60 content and the quenching was almost total. It is very well known that fullerene C60 quenches fluorescent species due its high electron affinity, its ability to

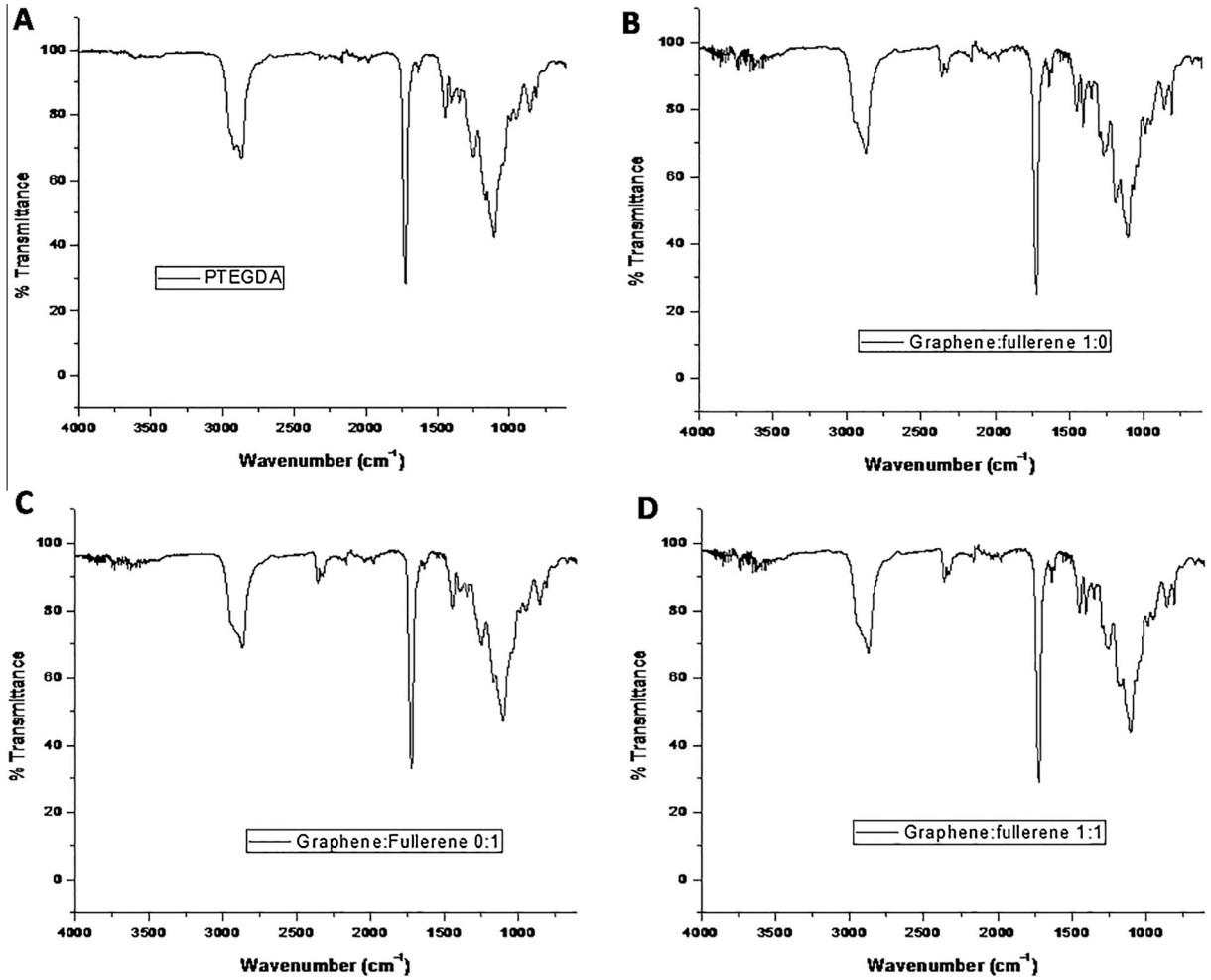

Fig. 4. FTIR spectra of: (A) sample FP(0/0); (B) sample FP(1/0); (C) sample FP(0/1) and (D) sample FP(1/1).

accept until 6 electrons in solution and its low reorganization energy. That is why it is very difficult to determine the exact quenching mechanism. However, it is highly possible that it occurs either via Fluorescence Resonance Energy Transfer (FRET) or electron transfer process. Electron transfer would be favored by the stabilization of the charged species by oligo(ethylene glycol) chains of the TEGDA matrix. Previously, our research group studied the quenching ability of fullerene in dendritic systems bearing pyrene, which is a very powerful fluorescent compound. Despite the high fluorescence of the pyrene chromophore, the presence of fullerene was able to quench it almost totally [54]. At present, there are no reports about the quenching of graphene emission using fullerene as quencher, because graphene is also employed as acceptor or quencher in systems exhibiting FRET or charge transfer [57]. However, a quenching effect that is similar to that observed in our samples was also reported in some composites of graphene with fluorescent organogelators. A decrease in the emission intensity of the composite was seen at higher graphene contents, modified by the presence of fullerene C60, which acted also as strong quencher preventing the aggregation [58]. On the other hand, there is no evidence of emission in samples containing only fullerene C60 at different amounts. This can be attributed to strong acceptor (quencher) character of fullerene and the sensitivity of its emission to the environment. This can be due to the sensitivity of fullerene emission to its environment. Emission could be quenched either by energy transfer, charge transfer, oxygen sensitization or triplet annihilation. Another possible fluorescence deactivation pathway is a charge transfer process with different donors present in the media.

The obtained hybrid materials were characterized by FTIR spectroscopy in the solid state. The incorporation of graphene and fullerene has been confirmed by this technique. From the practical point of view, there is no significant difference in the FTIR spectra of the samples obtained by frontal polymerization, batch polymerization or film casting.

As we can see in Fig. 4, the PTEGDA matrix shows a series of intense bands at 2925, 2886 (CH_2, str), 1721 (C═O, str) and 1098 (C—O, str) cm^{-1} due to the functional groups present in the polymer. Three weak bands were also observed in the region between 1455 and 1343 cm^{-1} due to bending vibrations. The spectrum of the sample FP(1/0) (B) exhibits the same bands present in the PTEGDA matrix accompanied by a discrete band at 1630 cm^{-1}, which is attributed to the C═C bonds present in graphene. The intensity of this band is quite weak due to the low content of graphene with respect to the polymer matrix. According to the literature, the FTIR spectrum of graphene shows two main bands at 1600 and 868 cm^{-1} [59]. Similarly, the FTIR spectrum of the sample FP(0/1) (C) exhibits also the characteristic bands of the polymer matrix. As reported in the literature, fullerene C60 shows four main bands [60] due to its icosohedral symmetry at 1428, 1180, 575 and 526 cm^{-1}, which are difficult to see since they are hidden by the bands of the polymer matrix. The last two bands can be observed only in the far infrared region. Finally, the FTIR spectrum of the FP(1/1) (D) is very similar to that of the sample containing only

graphene. However, if we compare the spectrum of the matrix with that of the nanocomposite samples, we can observe that in the former the band has a vibronic structure and shows a slight splitting at 2925, 2886 whereas in the latter it shows a well defined vibration band at 2925 cm^{-1}. A possible explanation is that the presence of the fullerene and graphene restrain the vibrational mobility of the CH_2 groups present in the oligo(ethylene glycol) segments of the PTEGDA matrix.

4. Conclusions

In this work, the dispersion of graphene and/or fullerene in a monomer (TEGDA) was accomplished by using a simple protocol that does not imply any chemical manipulation, thus preserving their pristine electronic structure [13]. This allowed us to directly polymerize the liquid monomer dispersion and to obtain the corresponding polymer nanocomposites. The polymerization was performed by classical and frontal polymerization. The corresponding materials were characterized by similar properties; however, FP was carried out in times that were much shorter than those needed for CP; namely, just a few minutes instead of 2 h. In addition, polymeric films were also prepared, which were used for extensive spectroscopic analyses. FTIR spectroscopy confirmed that graphene and fullerene C60 were incorporated into the nanocomposites. The optical properties of the nanocomposites were studied by absorption and fluorescence spectroscopy. Graphene-containing samples exhibited an absorption shoulder at 280 nm and showed significant fluorescence emission in the range between 600 and 800 nm, when they were excited at 280 nm. However, no emission was observed when the samples were excited at other wavelengths, so that we can conclude that fluorescence arises exclusively from graphene. Although, fullerene C60 usually shows an emission band at 780 nm, in the obtained nanocomposites containing this chromophore no emission was observed. This can be due to different deactivation pathways. A very efficient fluorescence quenching of graphene due to a FRET or charge transfer from graphene to fullerene C60 takes place. There is an evident stabilization of charge transfer species by the PTEGDA matrix.

References

[1] Geim AK, Novoselov KS. The rise of graphene. Nat Mater 2007;3:183–91.
[2] Zhang LL, Zhou R, Zhao XS. Graphene-based materials as supercapacitor electrodes. J Mater Chem 2010;29:5983–92.
[3] Rao CNR, Sood AK, Subrahmanyam KS, Govindaraj A. Graphene: the new two-dimensional nanomaterial. Angew Chem Int Ed 2009;42:7752–77.
[4] Tran NE, Lambrakos SG, Lagowski JJ. Analysis of capacitance characteristics of C60, C70, and La@C82. J Mater Eng Perform 2009;1:95–101.
[5] Barbieri O, Hahn M, Herzog A, Kotz R. Capacitance limits of high surface area activated carbons for double layer capacitors. Carbon 2005;6:1303–10.
[6] Hernandez Y, Nicolosi V, Lotya M, Blighe FM, Sun Z, De S, et al. High-yield production of graphene by liquid-phase exfoliation of graphite. Nat Nanotechnol 2008;3(9):563–8.
[7] Alzari V, Mariani A, Monticelli O, Valentini L, Nuvoli D, Piccinini M, et al. Stimuli-responsive polymer hydrogels containing partially exfoliated graphite. J Polym Sci Part A: Polym Chem 2010;48(23):5375–81.
[8] Alzari V, Nuvoli D, Scognamillo S, Piccinini M, Gioffredi E, Malucelli G, et al. Graphene-containing thermoresponsive nanocomposite hydrogels of poly(N-isopropylacrylamide) prepared by frontal polymerization. J Mater Chem 2011;21(24):8727–33.
[9] Nuvoli D, Valentini L, Alzari V, Scognamillo S, Bon SB, Piccinini M, et al. High concentration few-layer graphene sheets obtained by liquid phase exfoliation of graphite in ionic liquid. J Mater Chem 2011;21(10):3428–31.
[10] Scognamillo S, Gioffredi E, Piccinini M, Lazzari M, Alzari V, Nuvoli D, et al. Synthesis and characterization of nanocomposites of thermoplastic polyurethane with both graphene and graphene nanoribbon fillers. Polymer 2012;53(19):4019–24.
[11] Sanna R, Sanna D, Alzari V, Nuvoli D, Scognamillo S, Piccinini M, et al. Synthesis and characterization of graphene-containing thermoresponsive nanocomposite hydrogels of poly(N-vinylcaprolactam) prepared by frontal polymerization. J Polym Sci Part A: Polym Chem 2012;50(19):4110–8.
[12] Alzari V, Nuvoli D, Sanna R, Scognamillo S, Piccinini M, Kenny JM, et al. In situ production of high filler content graphene-based polymer nanocomposites by reactive processing. J Mater Chem 2011;21(41):16544–9.
[13] Coleman JN. Liquid exfoliation of defect-free graphene. Acc Chem Res 2012;46(1):14–22.
[14] Alzari V, Sanna V, Biccai S, Caruso T, Politano A, Scaramuzza N, et al. Tailoring the physical properties of nanocomposite films by the insertion of graphene and other nanoparticles. Composites: Part B 2014;60:29–35.
[15] Kim H, Macosko CW. Morphology and properties of polyester/exfoliated graphite nanocomposites. Macromolecules 2008;41(9):3317–27.
[16] Zhang K, Zhang LL, Zhao XS, Wu J. Graphene/polyaniline nanofiber composites as supercapacitor electrodes. Chem Mater 2010;22(4):1392–401.
[17] Eda G, Chhowalla M. Graphene-based composite thin films for electronics. Nano Lett 2009;9(2):814–8.
[18] Hong W, Xu Y, Lu G, Li C, Shi G. Transparent graphene/PEDOT–PSS composite films as counter electrodes of dye-sensitized solar cells. Electrochem Commun 2008;10(10):1555–8.
[19] Zhao L, Zhao L, Xu Y, Qiu T, Zhi L, Shi G. Polyaniline electrochromic devices with transparent graphene electrodes. Electrochim Acta 2009;55(2):491–7.
[20] Dang T, Hirsch L, Wantz G, Wuest JD. Controlling the morphology and performance of bulk heterojunctions in solar cells. Lessons learned from the benchmark poly(3-hexylthiophene):[6,6]-phenyl-C61-butyric acid methyl ester system. Chem Rev 2013;5:3734–65.
[21] Giacalone F, Martín N. Fullerene polymers: synthesis and properties. Chem Rev 2006;12:5136–90.
[22] Kamat PV, Turdy K, Baker DR, Radich JG. Beyond photovoltaics: semiconductor nanoarchitectures for liquid-junction solar cells. Chem Rev 2010;11:6664–88.
[23] Backer SA, Sivula K, Kavulak DF, Fréchet JMJ. High efficiency organic photovoltaics incorporating a new family of soluble fullerene derivatives. Chem Mater 2007;12:2927–9.
[24] Alley NJ, Liao KS, Andreoli E, Dias S, Dillon EP, Orbaek AW, et al. Effect of carbon nanotube-fullerene hybrid additive on P3HT:PCBM bulk-heterojunction organic photovoltaics. Synth Metals 2012;1–2(162):95–101.
[25] Ferguson AJ, Blackburn JL, Kopidakis N. Fullerenes and carbon nanotubes as acceptor materials in organic photovoltaics. Mater Lett 2013;90:115–25.
[26] Guldi DM, Prato M. Excited-state properties of C(60) fullerene derivatives. Acc Chem Res 2000;10:695–703.
[27] Kuramochi Y, Sandanayaka ASD, Satake A, Araki Y, Ogawa K, Ito O, et al. Energy transfer followed by electron transfer in a porphyrin macrocycle and central acceptor ligand: a model for a photosynthetic composite of the light-harvesting complex and reaction center. Chem Eur J 2009;9:2317–27.
[28] Bendikov M, Wudl F, Perepichka DF. Tetrathiafulvalenes, oligoacenenes, and their buckminsterfullerene derivatives: the brick and mortar of organic electronics. Chem Rev 2004;11:4891–946.
[29] Pérez E, Martín N. Curves ahead: molecular receptors for fullerenes based on concave–convex complementarity. Chem Soc Rev 2008;8:1512–9.
[30] Schuster DI, Li K, Guldi DM, Palkar A, Echegoyen L, Stanisky C, et al. Azobenzene-linked porphyrin–fullerene dyads. J Am Chem Soc 2007;51:15973–82.
[31] Imahori H, Sakata Y. Donor-linked fullerenes. Photoinduced electron transfer and its potential application. Adv Mater 1997;7:537–46.
[32] Araki Y, Ito O. Factors controlling lifetimes of photoinduced charge-separated states of fullerene-donor molecular systems. J Photochem Photobiol C: Photochem Rev 2008;3:93–110.
[33] Hahn U, Nierengarten JF, Vögtle F, Listorti A, Monti F, Armaroli N. Fullerene-rich dendrimers: divergent synthesis and photophysical properties. New J Chem 2009;2:337–44.
[34] Fiori S, Mariani A, Ricco L, Russo S. First synthesis of a polyurethane by frontal polymerization. Macromolecules 2003;8:2674–9.
[35] Chechilo NM, Khvilivitskii RJ, Enikolopyan NS. On the phenomenon of polymerization reaction spreading. Dokl Akad Nauk SSSR 1972;204:1180–1.
[36] Chechilo NM, Enikolopyan NS. Effect of pressure and initial temperature of the reaction mixture during propagation of a polymerization reaction. Dokl Phys Chem 1976;230:840–3.
[37] Pojman JA. Traveling fronts of methacrylic acid polymerization. J Am Chem Soc 1991;16:6284–6.
[38] Pojman JA, Varisli B, Perryman A, Edwards C, Hoyle C. Frontal polymerization with thiol-ene systems. Macromolecules 2004;3:691–3.
[39] Fortenberry DI, Pojman JA. Solvent-free synthesis of polyacrylamide by frontal polymerization. J Polym Sci Part A: Polym Chem 2000;7:1129–35.
[40] Pojman JA, Elcan W, Khan AM, Mathias L. Binary polymerization fronts: a new method to produce simultaneous interpenetrating polymer networks (SINs). J Polym Sci Part A Polym Chem 1997;2:227–30.
[41] Mariani A, Fiori S, Chekanov Y, Pojman JA. Frontal ring-opening metathesis polymerization of dicyclopentadiene. Macromolecules 2001;19:6539–41.
[42] Chen S, Tian Y, Chen L, Hu T. Epoxy resin/polyurethane hybrid networks synthesized by frontal polymerization. Chem Mater 2006;8:2159–63.
[43] Hu T, Chen S, Tian Y, Chen L, Pojman JA. Facile synthesis of poly (hydroxyethyl acrylate) by frontal free-radical polymerization. J Polym Sci Part A: Polym Chem 2007;5:873–81.
[44] Scognamillo S, Bounds C, Luger M, Mariani A, Pojman JA. Frontal cationic curing of epoxy resins. J Polym Sci Part A: Polym Chem 2010;9:2000–5.
[45] Gavini E, Mariani A, Rassu G, Bidali S, Spada G, Bonferoni MC, et al. Frontal polymerization as a new method for developing drug controlled release systems (DCRS) based on polyacrylamide. Eur Polym J 2009;3:690–9.

[46] Mariani A, Bidali S, Fiori S, Malucelli G, Sanna E. Self-ignition of polymerization fronts with convection: the rainstorm effect. E-polymers 2003;1:456–73.
[47] Scognamillo S, Alzari V, Nuvoli D, Mariani A. Thermoresponsive super water absorbent hydrogels prepared by frontal polymerization. J Polym Sci Part A: Polym Chem 2010;11:2486–90.
[48] Brunetti A, Princi E, Vicini S, Pincin S, Bidali S, Mariani A. Visualization of monomer and polymer inside porous stones by using X-ray tomography. Nucl Instrum Meth A 2004;1–2:235–41.
[49] Scognamillo S, Alzari V, Nuvoli D, Illescas J, Marceddu S, Mariani A. Thermoresponsive super water absorbent hydrogels prepared by frontal polymerization of N-isopropyl acrylamide and 3-sulfopropyl acrylate potassium salt. J Polym Sci Part A: Polym Chem 2011;2:1228–34.
[50] Mariani A, Fiori S, Bidali S, Alzari V, Malucelli G. Frontal polymerization of diurethane diacrylates. J Polym Sci Part A: Polym Chem 2008;10:3344–51.
[51] Scognamillo S, Alzari V, Nuvoli D, Mariani A. Hybrid organic/inorganic epoxy resins prepared by frontal polymerization. J Polym Sci Part A: Polym Chem 2010;21:4721–5.
[52] Illescas J, Sanna R, Alzari V, Nuvoli D, Casu M, Sanna R, et al. Organic–inorganic interpenetrating polymer networks and hybrid polymer materials prepared by frontal polymerization. J Polym Sci Part A: Polym Chem 2013;21:4618–25.
[53] Zaragoza-Galán G, Fowler MA, Duhamel J, Rein R, Solladié N, Rivera E. Synthesis and characterization of novel pyrene dendronized porphyrins exhibiting efficient fluorescence resonance energy transfer: optical and photophysical properties. Langmuir 2012;30:11195–205.
[54] Zaragoza-Galán G, Ortíz-Palacios J, Valderrama BX, Camacho-Dávila AA, Chávez-Flores D, Ramos-Sánchez VH, et al. Pyrene–fullerene C60 dyads as light-harvesting antennas. Molecules 2014;1:352–66.
[55] Zaragoza-Galán G, Fowler M, Rein R, Solladié N, Duhamel J, Rivera E. Fluorescence resonance energy transfer in partially and fully labeled pyrene dendronized porphyrins studied with model free analysis. J. Phys. Chem. C 2014;16:8280–94.
[56] Mariani A, Nuvoli D, Alzari V, Pini M. Phosponium-based ionic liquids as a new class of radical initiators and their use in gas-free frontal polymerization. Macromolecules 2008;14:5191–6.
[57] Ramakrishna Matte HSS, Subrahmanyam KS, Rao CNR. Synthetic aspects and selected properties of graphene. Nanomater Nanotechnol 2011;1:3–13.
[58] Samanta SK, Subrahmanyam KS, Bhattacharya S, Rao CNR. Composites of graphene and other nanocarbons with organogelators assembled through supramolecular interactions. Chem Eur J 2012;18:2890–901.
[59] Maka KF, Ju L, Wang F, Heinz TF. Optical spectroscopy of graphene: from the far infrared to the ultraviolet. Solid State Commun 2012;15:1341–9.
[60] Schettino V, Pagliai M, Ciabini L, Cardini G. The vibrational spectrum of fullerene C60. J Phys Chem A 2001;50:11192–6.